Analytical Model of Jet Shielding

Carl H. Gerhold*
Texas A&M University, College Station, Texas

An analytical model of the shielding of a stationary point noise source by a cylindrical jet is developed. The directivity function is derived which estimates the normalized sound pressure level at a far field receiver. The shielding model is compared to experimental data for a point noise source impinging on an unheated air jet and on a simulated hot air jet. The model compares favorably to measured shielding at receiver locations away from the jet axis. The trend of the estimated shielding diverges from the measured data as the jet axis is approached. Refinement of the model is discussed.

Introduction

ESTIMATION of aircraft generated noise includes identification not only of the sources of noise on the aircraft, but also of the propagation path between the source and receiver. One of the numerous factors affecting the noise transmission path is shielding of one jet by another. The shielding jet, because of the high temperature and flow speed with respect to the immediate surroundings, acts as a partial barrier between the source and the receiver. The resultant noise reduction not only affects the overall aircraft noise level, but also indicates the possibility of jet engine installation as a means of aircraft noise control.

The problem of reflection and transmission of sound by a moving medium has been addressed assuming a plane wave incident on a plane surface.[1-4] Ray tracing techniques have been applied to two-dimensional jets[5] and cold jets.[6] The two-dimensional formulation, for a cylindrical noise source impinging on the shielding jet has been developed.[7]

The present study is an extension to three dimensions of the previous analysis.[7] The model developed consists of the sound field emitted from a stationary, discrete frequency point source, which impinges on a cylinder of locally parallel flow. The temperature and velocity profiles are uniform in the jet at any location downstream of the nozzle. While this model is an idealization of the twin jet, it is felt to incorporate the basic elements essential for a realistic representation; not only of the source, but also of the shielding jet.

Model Development

Formulation of the Model

The mechanisms by which shielding occurs are reflection of sound at the boundary between the jet and the surrounding air and by diffraction around the jet. The noise source is modeled by a stationary discrete frequency point source located at $(r_0, 0,0)$. The shielding jet is a cylinder of radius a, and is infinite in extent along the z axis. The temperature and flow velocity are uniform across the cylinder cross section. The model is illustrated in Fig. 1. The expression for acoustic velocity potential is written for two regions; region I is outside the jet, region II is within the jet.

In region I (outside the flow)

$$\nabla^2\phi+\phi_{zz}-\frac{1}{c_0^2}\phi_{tt}=\frac{Q_0e^{-i\omega t}}{r}\delta(r-r_0)\delta(\theta)\delta(z) \tag{1}$$

In region II (inside the flow)

$$\nabla^2\phi+(1-M^2)\phi_{zz}-\frac{2M}{c_1}\phi_{zt}-\frac{1}{c_1^2}\phi_{tt}=0 \tag{2}$$

where ω is the source frequency, Q_0 the source strength, c the sound speed, M the Mach number (jet flow speed/c_1), δ the Dirac delta function, and

$$\nabla^2\phi=\phi_{rr}+\frac{1}{r}\phi_r+\frac{1}{r^2}\phi_{\theta\theta}$$

Note that the subscript 0 refers to condition outside the flow (ambient), and 1 refers to conditions within the heated jet.

The boundary conditions at the interface between the ambient air and the jet are as follows.

1) Sound pressure continuity

$$(p)_0=(p)_1 \text{ at } r=a \tag{3a}$$

or

$$-\rho_0(\phi_t)_0=-\rho_1(\phi_t+V\phi_z)_1 \text{ at } r=a \tag{3b}$$

where V = jet flow speed.

2) Continuity of the vortex sheet,[1,2] the condition which states that the displacement of the medium is continuous and symmetrical at the boundary; $r=a$. Denoting this displacement by $\eta=\eta(z,t)$, then,

$$\left.\frac{D\eta}{Dt}\right|_0=\left.\frac{D\eta}{Dt}\right|_1 \text{ at } r=a \tag{4a}$$

or

$$(\eta_t)_0=(\eta_t+V\eta_z)_1 \text{ at } r=a \tag{4b}$$

Time is eliminated from Eqs. (1) and (2) by assuming

$$\phi(r,\theta,z,t)=\psi(r,\theta,z)e^{-i\omega t}$$

The problem is reduced to a two-dimensional formulation by the Fourier transform

$$\tilde{\psi}=\frac{1}{2\pi}\int_{-\infty}^{+\infty}\psi e^{-ik_z z}dz$$

The transformed equations are as follows.

Region I

$$\nabla^2\tilde{\psi}+K_0^2\tilde{\psi}=\frac{Q_0}{2\pi r}\delta(r-r_0)\delta(\theta) \tag{5}$$

Presented as Paper 82-0051 at the AIAA 20th Aerospace Sciences Meeting, Orlando, Fla., Jan. 11-14, 1982; submitted Jan. 21, 1982; revision received June 18, 1982.

*Assistant Professor, Mechanical Engineering Department.

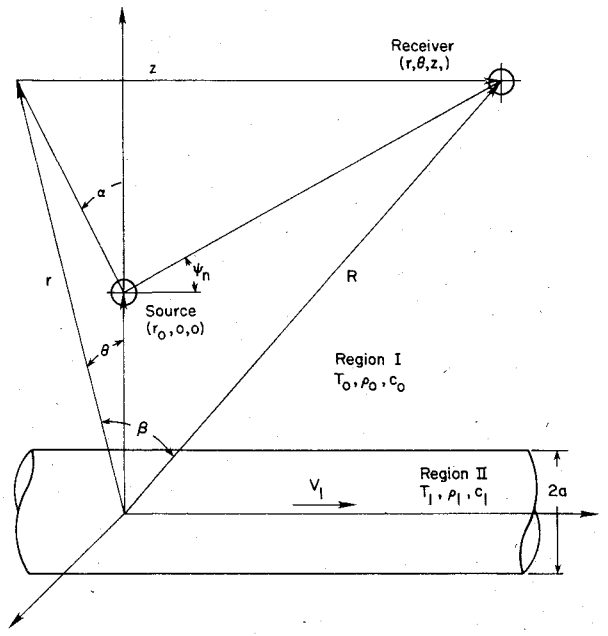

Fig. 1 Source-receiver geometry for jet shielding analysis.

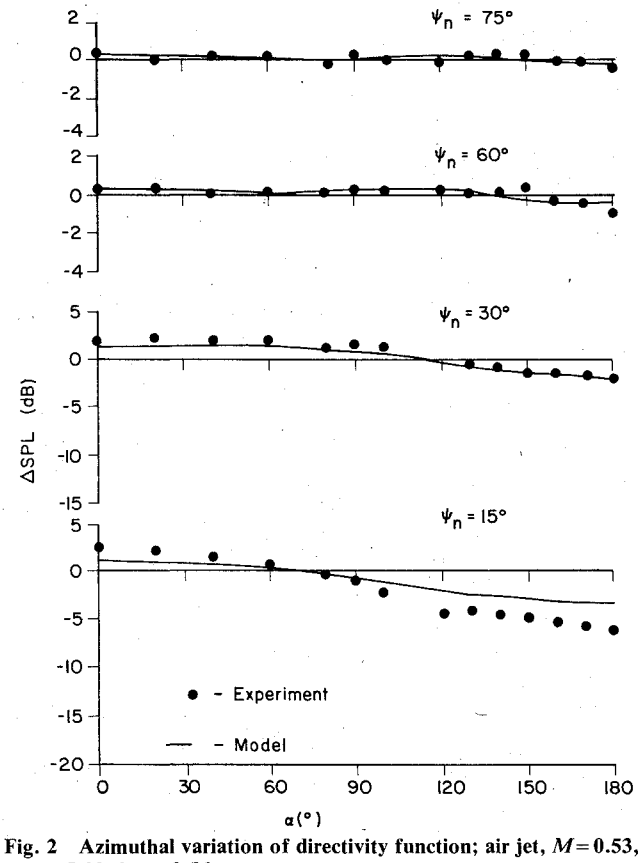

Fig. 2 Azimuthal variation of directivity function; air jet, $M=0.53$, $r_0/a=5.00$, $k_0a=0.56$.

Region II

$$\nabla^2\tilde{\psi}+K_1^2\tilde{\psi}=0 \tag{6}$$

where

$$K_0=[k_0^2-k_z^2]^{1/2} \qquad K_1=[k_1^2-k_z^2]^{1/2}$$

$$k_0=\omega/c_0 \qquad k_1=(\omega/c_1-Mk_z)$$

The solution of the wave equation in two dimensions for a source located at coordinates r_0 and 0 is shown in Ref. 8,

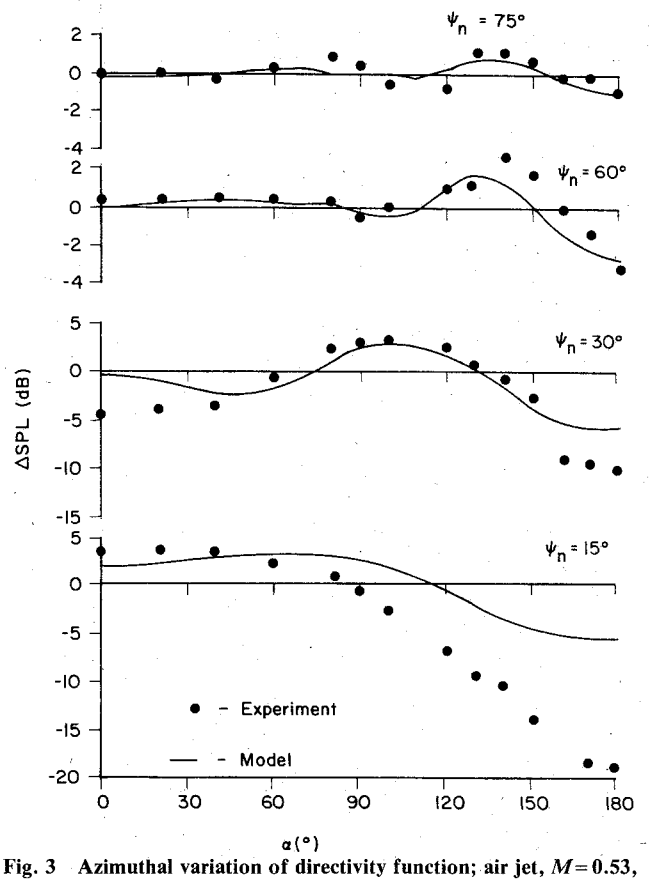

Fig. 3 Azimuthal variation of directivity function; air jet, $M=0.53$, $r_0/a=5.00$, $k_0a=1.60$.

Chap. 7. Thus, the solution of Eq. (5), describing the wave incident on the jet is

$$\tilde{\psi}_{\text{in}}=\frac{-iQ_0}{8\pi}\sum_{m=0}^{\infty}\epsilon_m\cos(m\theta)\times\begin{cases}J_m(K_0r)H_m(K_0r_0) & r<r_0\\ J_m(K_0r_0)H_m(K_0r) & r>r_0\end{cases} \tag{7}$$

where

$\epsilon_m=1 \quad m=0$

$\quad=2 \quad m\neq 0$

$J_m=$ Bessel function of the first kind of order m

$H_m=$ Hankel function of the first kind $=J_m+iY_m$

$Y_m=$ modified Bessel function of the first kind of order m

A wave is scattered into region I due to reflection from the jet. The scattered part is the solution of the homogeneous wave equation in region I, and has the form

$$\tilde{\psi}_{SC}=\sum_{m=0}^{\infty}A_m\cos(m\theta)H_m(K_0r) \tag{8}$$

where the Hankel function H_m is chosen to ensure that the wave is outgoing.

The solution of the wave equation for the wave transmitted into the jet is

$$\tilde{\psi}_{tr}=\sum_{m=0}^{\infty}B_m\cos(m\theta)J_m(K_1r) \tag{9}$$

where the Bessel function J_m is chosen to ensure that the solution is finite at the origin.

Inclusion of the boundary conditions and inverse transformation yields the equation for the acoustic velocity

potential in the far field ($r > r_0$)

$$\phi = \frac{-iQ_0 e^{-i\omega t}}{8\pi} \sum_{m=0}^{\infty} \epsilon_m \cos(m\theta) \times \int_{-\infty}^{+\infty} H_m(K_0 r) F_m(K_0, K_1) e^{ikz} dk_z \tag{10}$$

where

$$F_m(K_0, K_1) = J_m(K_0 r) - \left[\frac{H_m(K_0 r_0)[J_m(K_1 a) J'_m(K_0 a) - T J_m(K_0 a) J'_m(K_1 a)]}{T H_m(K_0 a) J'_m(K_1 a) - J_m(K_1 a) H'_m(K_0 a)} \right]$$

$$T = k_0^2 c_0^2 \rho_0 K_1 / k_1^2 c_1^2 K_0 \rho_1$$

Solution of the Model

An approximate solution of the integral in Eq. (10) is obtained using the method of stationary phase.[9] By this method, the solution of the integral I_z, of the form

$$I_z = \int_{-\infty}^{\infty} g(\alpha) e^{iz(h(\alpha))} d\alpha \text{ as } z \to \infty \tag{11}$$

is

$$I_z = \left[\frac{2\pi}{z\,|h''(\alpha_0)|} \right]^{1/2} g(\alpha_0) \exp[i(z(h(\alpha_0)) \pm \pi/4)]$$

where 1) α_0 solves $h'(\alpha) = 0$ and 2) the sign in the exponential term goes as the sign of $h''(\alpha_0)$. In order to solve Eq. (10) in the manner prescribed by Eq. (11), the following transformation is made. Let

$$\alpha = (1 - (k_z/k_0)^2)^{1/2}$$

The integral in Eq. (10) becomes

$$I = -k_0 \int_{-\infty}^{+\infty} \frac{\alpha e^{ik_0 z\sqrt{1-\alpha^2}}}{\sqrt{1-\alpha^2}} \{Hm(k_0 r\alpha) F_m(\alpha) d\alpha\} \tag{12a}$$

In the acoustic far field, $r \gg 1$. For values of k_0 such that $k_0 r \gg 1$, and assuming $k_z \ll k_0$ such that $\alpha \approx 1$, the argument of the Hankel function $k_0 r\alpha \gg 1$ and the large argument approximation of the Hankel function applies.[10] From Fig. 1, it is seen that

$$r = R\cos\beta \quad \text{and} \quad z = R\sin\beta$$

The integral is then

$$I = -\left(\frac{2k_0}{\pi R\cos\beta} \right)^{1/2} \exp\left[-i\frac{\pi}{2}(m + 1/2) \right] \times \int_{-\infty}^{\infty} \left(\frac{\alpha}{1-\alpha^2} \right)^{1/2} \times F_m(\alpha) \exp(ik_0 R(\alpha\cos\beta + \sqrt{1-\alpha^2}\sin\beta)) d\alpha \tag{12b}$$

The term $h(\alpha)$ is

$$h(\alpha) = \sqrt{1-\alpha^2}\sin\beta + \alpha\cos\beta$$

from which solution for α_0 yields

$$\alpha_0 = \cos\beta$$

Thus, the expression for the total far field acoustic velocity potential is

$$\phi_T = \frac{Q_0 e^{-i\omega t}}{4\pi R} \sum_{m=0}^{\infty} \epsilon_m \cos(m\theta) e^{-i\frac{m\pi}{2}} e^{ik_0 R} F_m(\cos\beta) \tag{13}$$

where

$$F_m(\cos\beta) = J_m(k_0 r_0 \cos\beta) - \{ H_m(k_0 r_0 \cos\beta) [\rho_1 c_1 T_1^2 \cos(\beta) J_m(k_0 a T_2) J'_m(k_0 a \cos\beta) - \rho_0 c_0^2 T_2 J_m(k_0 a\cos\beta) J'_m(k_0 a T_2)] \div [\rho_1 c_1^2 T_1^2 \cos\beta J_m(k_0 a T_2) H'_m(k_0 a\cos\beta) - \rho_0 c_0^2 T_2 H_m(k_0 a\cos\beta) J'_m(k_0 a T_2)] \} \tag{14}$$

$$T_1 = (c_0/c_1) - M\sin\beta$$

$$T_2 = \left[\left(\frac{c_0}{c_1} - M\sin\beta \right)^2 - \sin^2\beta \right]^{1/2}$$

The total acoustic velocity potential consists of the incident and the scattered waves, and is characterized by the terms in Eq. (14). The incident wave is:

$$\phi_{\text{in}} = \frac{Q_0 e^{-i\omega t}}{4\pi R} \sum_{m=0}^{\infty} \epsilon_m \cos(m\theta) e^{-i\frac{m\pi}{2}} e^{ik_0 R} J_m(k_0 r_0 \cos\beta) \tag{15}$$

and the scattered part is represented by the terms within the brackets in Eq. (14).

Results

The sound pressure is evaluated from the acoustic velocity potential by

$$P = -\rho_0 \frac{\partial}{\partial t} \phi$$

The total sound pressure P_T at a receiver location in the acoustic far field is evaluated from Eq. (13). The incident sound pressure P_{in} is evaluated from Eq. (15). The normalized sound pressure level is expressed as a directivity function ΔSPL, where

$$\Delta\text{SPL} = 10\log \left| \frac{P_T}{P_{\text{in}}} \right|^2 (\text{dB})$$

ΔSPL > 0 indicates amplification and ΔSPL < 0 indicates sound level reduction.

Measurements of the sound pressure level from a point source near a jet have been made by Yu and Fratello at NASA Langley Research Center.[11] For the purposes of testing the analytical model, comparison of the measured shielding to the shielding estimated by the model are made. Test cases include an unheated Mach number 0.53 air jet and a simulated hot air Mach 0.18 jet using helium as the flow medium. In the experiments, the noise source is located 4 jet diameters downstream of the shielding jet nozzle exit. The jet diameter is 25.4 mm and the lateral spacing between the source and the center of the jet is 2.5 jet diameters. The receiver is in the acoustic far field, $R = 120$ jet diameters.

The coordinates are shifted to a set centered on the sound source, and are illustrated in Fig. 1. In the nomenclature adopted for the comparison, $\psi_n = 0$ deg on the z axis of the source, parallel to the shielding jet. The angle α is 0 deg when the receiver is on the source side of the jet, and 180 deg when the receiver is directly opposite the jet from the source.

Unheated, Subsonic Jet

Figures 2 and 3 show the modification of the directivity function by the shielding jet in azimuthal planes downstream of the source. The curves in Fig. 2 are for the normalized frequency parameter, $k_0 a = 0.56$, where k_0 is the wavenumber

equal to $2\pi f/c_0$ and a is the shielding jet radius. Figure 3 is for $k_0a=1.6$.

At low frequency, Fig. 2, the shielding effect is small. At the near downstream location, $\psi_n=75$ deg, incident sound is transmitted through the jet, and backscattering is negligible. As the receiver moves downstream from the source, the shadow zone, in which ΔSPL is less than zero, becomes more well defined. The zone becomes wider and the maximum attenuation increases as the jet axis is approached ($\psi_n\to 0$ deg). The sound is scattered into a lobe immediately adjacent to the zone.

At higher frequency, Fig. 3, the broadening of the shadow zone is less, but the maximum attenuation is greater. The lobe of amplification adjacent to the shadow zone shifts toward the source side of the shielding jet and becomes wider as the jet axis is approached.

The trends exhibited by the model compare favorably with experiment for both low and high frequency. The measured data show lobe formations similar to those estimated. The model underestimates the maximum sound reduction in the shadow zone at receiver locations near the jet axis ($\psi_n<30$ deg). The discrepancy increases with frequency.

The directivity function is evaluated on the side of the jet directly opposite the source, for $\psi_n<90$ deg (downstream of the source) and $\psi_n>90$ deg (upstream of the source), and is shown in Fig. 4.

Sound is scattered into the region upstream of the source, $\psi_n>90$ deg, and the magnitude of the amplification increases with frequency. As the receiver moves downstream from the source, $\psi_n<90$ deg, sound is attenuated. The rate of sound reduction is at first gradual, and then increases at the angle $\psi_n\approx 50$ deg. For angles with the range 90 deg$>\psi_n>50$ deg transmission of noise through the jet is dominant.

The transmission cutoff angle

$$\psi_{nct}=\cos^{-1}\left(\frac{c_0/c_1}{1+M}\right)$$

is the angle greater than which, theoretically, all sound is transmitted, and less than which no transmission through the jet occurs.[4] In the model development of the previous section, ψ_{nct} is the angle at which the parameter T_2 goes to zero in Eq. (14).

$$T_2=\left[\left(\frac{c_0}{c_1}-M\cos\psi_n\right)^2-\cos^2\psi_n\right]^{1/2}=0 \text{ at } \psi_n=\psi_{nct}$$

where

$$\psi_n\cong(\pi/2)-\beta$$

for the operating parameters $\psi_{nct}=49$ deg. From Fig. 4, sound continues to transmit through the jet at $\psi_n<\psi_{nct}$. However, the dominance of sound transmission decreases as more sound is refracted downstream in the jet.

As the jet axis is approached, ($\psi_n\to 0$), and the transmitted sound contribution diminishes, sound diffracted around the jet becomes dominant. This diffracted sound imposes a theoretical limit on the shielding of approximately 6 dB.

The analytical results show agreement in form with the experimental results. The model underestimates the magnitude of sound scattering upstream of the source. The model follows closely the trend of the measured data in the transmission dominant zone. As the jet axis is approached, the measured sound level continues to decrease; while the model approaches a sound reduction limit. This indicates that diffraction is a less dominant mechanism in shielding by a real jet.

Simulated Hot, Subsonic Jet

The purpose for development of the model is to estimate the shielding for heated jets. For this reason, the model is compared to a simulated hot jet using helium as the flow medium. In this jet, the density ratio $\rho_1/\rho_0=1/7$ and the sound speed ratio $c_1/c_0=3.0$. The jet Mach number $V/c_1=0.18$.

Figure 5 shows the directivity function on the side of the jet opposite the source at the normalized frequencies, k_0a, of 0.56 and 1.6. The curves are similar to the unheated jet, Fig. 4. Unlike the unheated jet, the directivity function is less than

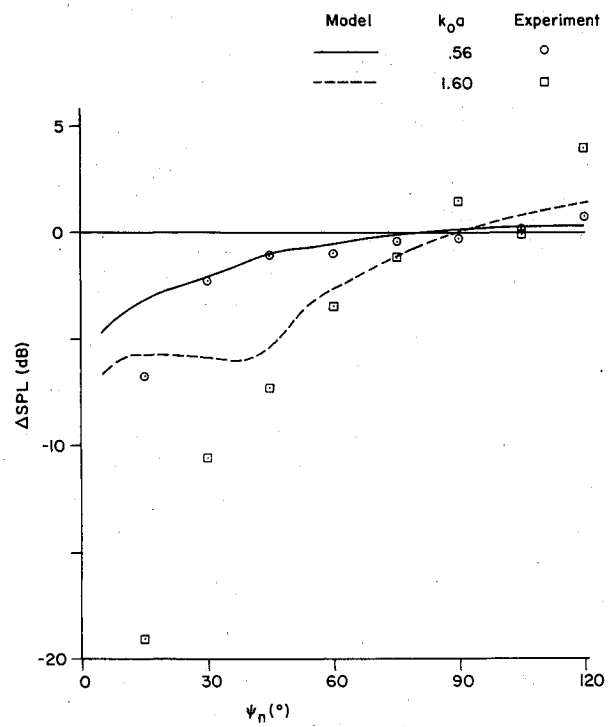

Fig. 4 Polar variation of directivity function; air jet, $M=0.53$, $r_0/a=5.00$, $\alpha=180$ deg.

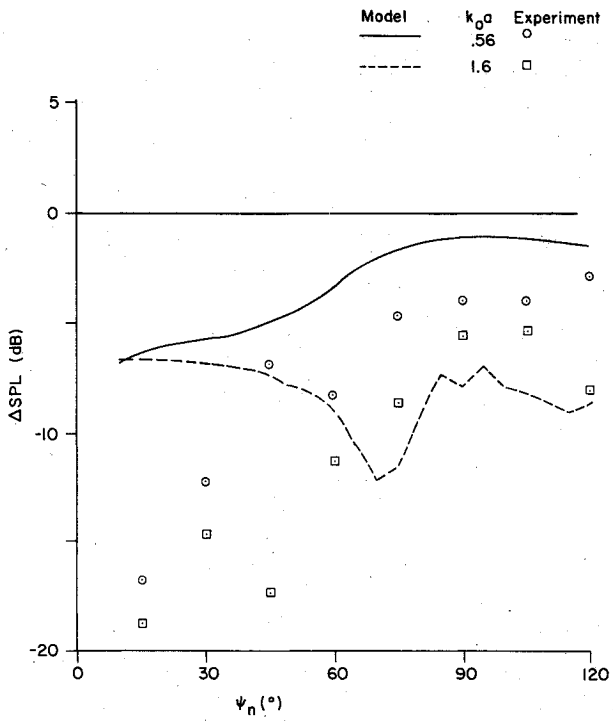

Fig. 5 Polar variation of directivity function; helium jet, $M=0.18$, $r_0/a=5.00$, $\alpha=180$ deg.

zero upstream of the source. This indicates that the density difference between the ambient air and the jet stream increases scattering toward the source side of the shielding jet.

The model estimates the trend of the experimental data for upstream locations, showing sound reduction upstream of the noise source. The model follows the trend of the data in the near downstream region. As with the unheated jet, the experiment shows less influence of diffraction farther downstream than does the model.

Conclusions

The model estimates the trend of shielding, not only on the side of the jet opposite the source, but also in the azimuthal planes downstream of a source impinging on the unheated jet. It is in the region near the jet axis that the trend of the experimental data diverges from the model. The model shows a greater dependence on the diffraction of sound. Continuing model development is addressing resolution of this discrepancy. The shielding jet is modeled as an infinite cylinder of constant cross section, where the actual jet widens downstream. As the jet widens, it becomes more effective as a sound barrier. Thus, less sound is diffracted into the shadow zone on the side of the jet opposite the jet opposite the source. From barrier theory, the scattering effect is more pronounced as the frequency increases. Thus, the jet widening alters the diffracted noise pattern more at high frequency than at low frequency. Preliminary results have been obtained with the jet model modified to include a widening algorithm. The results indicate that inclusion of the jet widening can resolve, in large part, the discrepancies between the model and experiment.

Acknowledgments

This work is supported by NASA Langley Research Center under Grant NAG-1-11. The author is indebted to Dr. J. C. Yu of the Aeroacoustics Branch and to personnel of the Noise Prediction Group for their assistance in the conduct of this research.

References

[1] Ribner, H. S., "Reflection, Transmission, and Amplification of Sound by a Moving Medium," *Journal of the Acoustical Society of America*, Vol. 29, April 1957, p. 435.

[2] Miles, J. W., "On the Reflection of Sound at an Interface of Relative Motion," *Journal of the Acoustical Society of America*, Vol. 29, Feb. 1957, p. 226.

[3] Yeh, C., "Reflection and Transmission of Sound Waves by a Moving Fluid Layer," *Journal of the Acoustical Society of America*, Vol. 41, April 1957, p. 817.

[4] Yeh, C., "A Further Note of the Reflection and Transmission of Sound Waves by a Moving Fluid Layer," *Journal of the Acoustical Society of America*, Vol. 43, June 1968, p. 1454.

[5] Parthasarathy, S. P., Cuffel, R. F., and Massier, P. F., "Twin Jet Study, Final Report," Jet Propulsion Laboratory, California Institute of Technology, Pasadena, Calif., Nov. 3, 1978, pp. 1-51.

[6] Candel, S. and Julienne, A., "Shielding and Scattering by a Jet Flow," AIAA Paper 76-545, July 1976.

[7] Gerhold, C. H., "Two-Dimensional Analytical Model of Twin Jet Shielding," *Journal of the Acoustical Society of America*, Vol. 69, April 1981, p. 904.

[8] Morse, P. and Ingard, P., *Theoretical Acoustics*, McGraw-Hill, New York, 1968.

[9] Jefferies, H. and Jefferies, B., *Methods of Mathematical Physics*, Cambridge University Press, 1956.

[10] Abramowitz, M. and Stegun, J., *Handbook of Mathematical Functions*, Dover Press, New York, 1965.

[11] Yu, J. C. and Fratello, D. J., "Measurements of Acoustic Shielding by a Turbulent Jet," AIAA Paper 81-2019, Oct. 1981.